Developmental Biology 346 (2010) 128–139

Contents lists available at ScienceDirect

Developmental Biology

journal homepage: www.elsevier.com/developmentalbiology

Evolution of Developmental Control Mechanism

Conserved mechanism of Wnt signaling function in the specification of vulval precursor fates in *C. elegans* and *C. briggsae*

Ashwin Seetharaman [1,2], Philip Cumbo [1], Nagagireesh Bojanala [3], Bhagwati P. Gupta *

Department of Biology, McMaster University, Hamilton, ON, Canada L8S 4K1

ARTICLE INFO

Article history:
Received for publication 9 February 2010
Revised 17 June 2010
Accepted 1 July 2010
Available online 17 July 2010

Keywords:
Nematode
C. elegans
C. briggsae
Vulval development
Signal transduction
Wnt signaling

ABSTRACT

The *C. elegans* hermaphrodite vulva serves as a paradigm for understanding how signaling pathways control organ formation. Previous studies have shown that Wnt signaling plays important roles in vulval development. To understand the function and evolution of Wnt signaling in *Caenorhabditis* nematodes we focused on *C. briggsae*, a species that is substantially divergent from *C. elegans* in terms of the evolutionary time scale yet shares almost identical morphology. We isolated mutants in *C. briggsae* that display multiple pseudo-vulvae resulting from ectopic VPC induction. We cloned one of these loci and found that it encodes an Axin homolog, Cbr-PRY-1. Our genetic studies revealed that *Cbr-pry-1* functions upstream of the canonical Wnt pathway components *Cbr-bar-1* (*β-catenin*) and *Cbr-pop-1*(*tcf/lef*) as well as the Hox target *Cbr-lin-39* (*Dfd/Scr*). We further characterized the *pry-1* vulval phenotype in *C. briggsae* and *C. elegans* using 8 cell fate markers, cell ablation, and genetic interaction approaches. Our results show that ectopically induced VPCs in *pry-1* mutants adopt 2° fates independently of the gonad-derived inductive and LIN-12/Notch-mediated lateral signaling pathways. We also found that *Cbr-pry-1* mutants frequently show a failure of P7.p induction. A similar, albeit low penetrant, defect is also observed in *C. elegans pry-1* mutants. The genetic analysis of the P7.p induction defect revealed that it was caused by altered regulation of *lin-12* and its transcriptional target *lip-1* (MAP kinase phosphatase). Thus, our results provide evidence for LIN-12/Notch-dependent and independent roles of Wnt signaling in promoting 2° VPC fates in both nematode species.

Introduction

Multicellular organisms have evolved complex cell communication machinery that enables cells to recognize and respond to a diverse range of extracellular signals. This interaction is crucial for the survival of organisms and their ability to function as coherent systems. Communication between cells and their environment is mediated by receptors that interact with specific ligands to transduce the signal into the cell. This leads to the activation of a cascade of intracellular proteins, many of which are components of a relatively small set of evolutionarily conserved signaling pathways, such as Ras, Notch, and Wnt (Bray, 2006; Eisenmann, 2005; Logan and Nusse, 2004; Sundaram, 2005). Among these, the Wnt signaling pathway has been shown to control diverse developmental processes including cell proliferation, cell polarity, and cell migration (Eisenmann, 2005; Widelitz, 2005). Studies on Wnt signaling have identified several genes that encode pathway components such as Wnt (ligand), Frizzled (receptor) and β-Catenin (transcriptional regulator). Analysis of their function has revealed that in normal cells, in the absence of Wnt ligands, β-Catenin is actively degraded by the action of a protein complex that contains scaffolding proteins Axin and APC and a serine/threonine kinase GSK3β (Logan and Nusse, 2004). The interaction of Wnts with Frizzled receptors activates the pathway leading to the dissociation of this complex, allowing cytoplasmic β-Catenin to translocate to the nucleus and interact with the TCF/LEF factor to regulate gene transcription.

The nematode *C. elegans* is a leading model organism to understand the mechanism of Wnt signaling function in development. Genetic studies in *C. elegans* have shown that Wnt signaling controls multiple processes including embryonic patterning, gonadogenesis, neuronal differentiation, male hook formation, and vulval development (Eisenmann and Kim, 2000; Eisenmann et al., 1998; Gleason et al., 2002; Maloof et al., 1999; Rocheleau et al., 1997; Salser and Kenyon, 1992; Siegfried and Kimble, 2002; Sternberg and Horvitz, 1988; Thorpe et al., 1997; Yu et al., 2009). The downstream targets of the pathway include three Hox genes, *lin-39 (Deformed/Sex combs reduced (Dfd/Scr) family)*, *mab-5 (Antennapedia/Ultrabithorax/abdominal-A (Antp/Ubx/Abd-A) family)* and *egl-5 (Abdominal-B (Abd-B) family)* that are expressed in multiple tissues and control diverse cell fates (Eisenmann, 2005; Kenyon et al., 1997).

Due to its simplicity, the *C. elegans* vulva has been successfully used to study the regulation and function of Wnt signaling pathway

* Corresponding author. Fax: +1 905 522 6066.
E-mail address: guptab@mcmaster.ca (B.P. Gupta).
[1] Co-first authors.
[2] Present address: University of Toronto, Ontario, Canada.
[3] Present address: Biology Center, ASCR, Institute of Parasitology, Budweis, Czech Republic, 37005.

0012-1606/$ – see front matter © 2010 Elsevier Inc. All rights reserved.
doi:10.1016/j.ydbio.2010.07.003

components. The vulva develops from three of six ventral hypodermal cells (termed P3.p to P8.p) that escape fusion to the surrounding hypodermal syncytium, hyp7, during the L1 stage and become vulval precursor cells (VPCs). This process is mediated by *lin-39* since all Pn.p cells in *lin-39* mutants fuse to hyp7 in the L1 stage. The *lin-39* activity is also required during the L2 stage to prevent VPCs from fusing to hyp7, and maintaining their competence to respond to patterning signals. The L2-stage expression of *lin-39* is positively regulated by the BAR-1 (β-Catenin)-mediated canonical Wnt signaling pathway. In *bar-1* mutants *lin-39* activity is greatly reduced which causes VPCs to inappropriately fuse with hyp7 (Eisenmann et al., 1998). The other Wnt pathway components that regulate VPC competence include 5 Wnt ligands (LIN-44, CWN-1, CWN-2, EGL-20, and MOM-2), 3 Frizzled receptors (LIN-17, MOM-5, and MIG-1), PRY-1 (Axin), and POP-1 (TCF/LEF) (Eisenmann, 2005; Gleason et al., 2002; Gleason et al., 2006; Inoue et al., 2004). The expression analysis of Wnt pathway genes has revealed that multiple tissues could act as sources of Wnt signals (including gonad, muscles, and many cells in the tail region) (Gleason et al., 2006; Herman et al., 1995; Inoue et al., 2004; Whangbo and Kenyon, 1999). The finding that Wnt ligands form anteroposterior gradient and pattern certain cell fates (Coudreuse et al., 2006) provides support to a model that similar signals originating from non-vulval tissues may differentially affect VPC fates.

In addition to Wnt, VPCs also respond to inductive signaling initiated by the LIN-3/Epidermal Growth Factor (EGF) ligand and lateral signaling via the LIN-12/Notch receptor (Greenwald, 2005; Sternberg, 2005). The LIN-3/EGF, secreted by a gonadal anchor cell (AC), interacts with the LET-23/EGF receptor and initiates a MPK-1/MAP kinase-mediated signaling pathway in VPCs. This causes P6.p to adopt a 1° fate. The interactions between P(5-7).p, mediated by LIN-12/Notch lateral signaling, confers a 2° fate on P5.p and P7.p. The induced VPCs, P(5-7).p, divide during L3/L4 stages to generate 22 progeny that differentiate to form 7 different cell types (vulA to vulF) (Sharma-Kishore et al., 1999). The remaining uninduced VPCs (P3.p, P4.p and P8.p) adopt a 3° fate and fuse to hyp7. The presence of various regulators of the signaling pathways, genetic redundancies, as well as crosstalks between pathways, ensures that a 3°-3°-2°-1°-2°-3° spatial pattern is reproducibly generated.

The simplicity and ease of experimental manipulations of the vulva has facilitated comparative developmental analysis among nematode species. These findings have revealed similarities and differences in some of the underlying developmental mechanisms (Eizinger and Sommer, 1997; Felix, 2005, 2007; Sommer, 2005; Sommer and Sternberg, 1996; Tian et al., 2008; Zheng et al., 2005). For example, the *lin-17*/*Frizzled* receptor ortholog in *Pristionchus pacificus* represses vulval cell fates, whereas in *C. elegans lin-17* promotes VPC competence and cell fates (Eisenmann, 2005; Zheng et al., 2005). The *P. pacificus* and *Oscheius tipulae lin-39* orthologs represent another case of evolutionary conservation and divergence of gene function. While the *O. tipulae lin-39* promotes VPC competence similar to *lin-39* in *C. elegans* (Louvet-Vallee et al., 2003), the *P. pacificus lin-39* prevents VPCs from undergoing programmed cell death (Eizinger and Sommer, 1997).

Among the species that are closely related to *C. elegans*, *C. briggsae* is used extensively in comparative studies (Gupta et al., 2007). Although the two species diverged roughly 30 million years ago (Cutter, 2008), morphologically they appear very similar. This provides a unique opportunity to study gene function and signaling pathways in specifying homologous processes. We are taking a forward genetics approach to study the mechanism of vulval development in *C. briggsae*. This work focuses on *pry-1* (*Axin* family) and its interactions with Wnt and LIN-12/Notch signaling pathway components in VPC fate specification. We found that the *Cbr-pry-1* mutants display a unique pattern of vulval induction defect that is characterized by ectopically induced P3.p, P4.p, and P8.p, and an uninduced P7.p. The genetic analysis of *Cbr-pry-1* interaction with other genes revealed that *Cbr-bar-1 (β-catenin)-Cbr-pop-1 (tcf/lef)*-mediated canonical Wnt signaling plays an essential role in promoting VPC competence and cell proliferation in *C. briggsae*. The downstream targets of the pathway include the *Hox* gene *Cbr-lin-39*. To understand the mechanism of *pry-1*-mediated Wnt signaling function we used a combination of cell fate markers, laser microsurgery, and genetic interaction experiments. The findings show that ectopically induced VPCs in *pry-1* mutants, in both *C. elegans* and *C. briggsae,* acquire 2° fate independently of the gonad-derived inductive signaling and LIN-12/Notch-mediated lateral signaling pathways. However, interestingly, in the case of P7.p our data suggests that *pry-1* acts genetically upstream of *lin-12* and its transcriptional target *lip-1* to promote vulval cell fate. Taken together these findings reveal that Wnt signaling utilizes multiple mechanisms to specify the spatial pattern of VPC fates in *C. elegans* and *C. briggsae*.

Materials and Methods

Strains and general methods

The general methods for culturing and genetic manipulations have been previously described (Brenner, 1974). All experiments were carried out at 22 °C unless otherwise noted. The staging of animals was primarily based on the gonad morphology as described in Wormatlas (Hall and Altun, 2008). The gonad arms initiate turning during mid-L3 stage and by mid-L4 stage arms are in close proximity to the center of vulval invagination formed by P(5-7).p progeny.

Various mutations used in this study are listed below in the alphabetical order. Where known, the locations of mutations and transgenic strains are indicated. The '*Cbr*' prefix denotes the *C. briggsae* ortholog of a *C. elegans* gene.

C. briggsae: AF16 (wild type), *Cbr-pry-1 (sy5353) I, Cbr-pry-1 (sy5270) I, Cbr-pry-1(sy5411) I, Cbr-unc-119(st20000) III, mfIs5[Cbr-egl-17::GFP, myo-2::GFP], mfIs8[Cbr-zmp-1::GFP, myo-2::GFP], mfIs29 [lip-1::GFP, myo-2::GFP], mfEx33[dlg-1::GFP, myo-2::dsRed], mfIs42[sid-2(+), myo-2::dsRed], bhEx59[hsp::Cbr-pry-1, myo-2::GFP], bhEx83[Cbr-pry-1-5 kb::GFP, unc-119(+)], bhEx84[Cbr-pry-1-3.8 kb::GFP, unc-119 (+)].*

C. elegans: N2 (wild type), *lin-12(n137) III, lin-12(n952) III, lin-12 (n676n909) III, lip-1(zh15) IV, pop-1(hu9) I, pry-1(mu38) I, unc-119 (ed4) III, ayIs4[egl-17::GFP, dpy-20(+)] I, bhEx53[daf-6::YFP, myo-2::GFP], deIs4[dpy-20(+), ajm-1::GFP, lin-39TX::GFP (yeast DNA)], muIs32 [mec-7::GFP] II, syIs54[ceh-2::GFP, unc-119(+)] II, syIs80[lin-11::GFP, unc-119(+)] III, syIs101[dhs-31::GFP, unc-119(+)] IV, wyEx3372[syg-2::GFP], zhIs4[lip-1::GFP, unc-119(+)] III.*

The transgenic animals carrying extrachromosomal arrays were generated by standard microinjection technique (Mello et al., 1991) using *C. elegans unc-119* (Maduro and Pilgrim, 1995) and *myo-2::GFP* (pPD118.33) (S. Q. Xu, B. Kelly, B. Harfe, M. Montgomery, J. Ahnn, S. Getz and A. Fire, personal communication) as transformation markers. The concentrations of plasmids that were injected as part of this study are: *hsp::Cbr-pry-1* 25 ng/μl, *Cbr-pry-1::GFP* (each of 3.8 kb and 5 kb promoter fragment) 100 ng/μl, *daf-6::YFP* 100 ng/μl.

The synchronized L1 stage *hsp::Cbr-pry-1* animals were heat shocked at 31 °C for 24 hrs and subsequently grown at 22 °C until adulthood. Cell ablation experiments were performed as described (Avery and Horvitz, 1987). The gonad precursors (Z1 to Z4) were ablated during the L1 stage whereas VPCs were ablated during the L2 stage. Worms were recovered from slides and allowed to grow until L4 stage. Vulval phenotypes were examined using Nomarski optics.

Vulval phenotype and induction analysis

We scored VPC competence and induction during the L2-L4 stages. A VPC was considered induced if it gave rise to 4 or more progeny that had invaginated. With the exception of P7.p and P8.p in *pry-1* mutants

that appear morphologically similar to P12.pa (referred as P12.pa-like fate), an uninduced VPC can adopt either an F fate (no division and fusion to hyp7 syncytium in L2) or a 3° fate (one division followed by fusion of both daughters to hyp7 in L3). In wild-type animals (*C. elegans* and *C. briggsae*) P4.p and P8.p always adopt a 3° fate, while P3.p does in ~20°-50% of cases (F fate in the remainder). Statistical analyses were performed using InStat 2.0 (GraphPad) Software. Two-tailed P values were calculated in unpaired t tests and values less than 0.05 were considered statistically significant.

Unlike wild type animals in which P3.p, P4.p and P8.p fuse to hyp7, in *pry-1* mutants these Pn.p cells can be ectopically induced to divide (termed 'Overinduced'). Additionally, *pry-1* mutants frequently show a failure of P7.p induction (termed 'Underinduced'). Thus, the same animal can exhibit both Overinduced and Underinduced phenotypes.

Isolation and mapping of C. briggsae pry-1

The *Cbr-pry*-1 mutants were isolated in a genetic screen for animals that exhibit defects in vulval induction. Wild-type L4 stage AF16 animals were fed with 25 mM Ethyl Methanesulfonate (EMS; Sigma) for 3 hrs using standard procedures (Wood, 1988). More than 500,000 haploid genomes were screened and F2 animals showing multiple pseudo-vulvae were isolated. Putative lines that showed a reproducible phenotype were retained and backcrossed three to four times.

The complementation and linkage studies revealed that three mutants *sy5270, sy5353* and *sy5411* define a locus on LG*I* and map close to a levamisole-resistant mutant *lev(sy5440)* (*www.briggsae.org*). Subsequently, polymorphism (insertion-deletion or indel)-based mapping (using HK104 isolate) was used to determine the physical location of *sy5353*. The indels were computationally identified and validated by PCR amplification of roughly 250 bp flanking sequences and analyzed by agarose gel electrophoresis (Koboldt et al., 2010). Of the five Chromosome I indels, *bhP1* (fpc3441), *bhP7* (fpc4171), *bhP19* (fpc2695), *bhP29* (fpc4140) and *bhP42* (fpc4184), three (*bhP1, bhP7* and *bhP42)* showed strong linkage to *sy5353* (based on band intensities of PCR amplified DNA on 4% Invitrogen UltraPure Agarose 1000). The *bhP29* was weakly linked (Figs. 1A and S1, data not shown) whereas *bhP19* showed no linkage to *sy5353*. We also recovered recombinants between *sy5353, bhP1* and *bhP42* and determined that *sy5353* maps 2 mu away from *bhP1* (1 recombinant out of the total 46 chromosomes tested) whereas *bhP1* and *bhP42* are 5 mu apart (3 recombinants out of the total 60 chromosomes tested). A search for the *C. elegans* orthologs in *C. briggsae* genome (CB3 assembly) identified *Cbr-pry-1* as a candidate gene that is ~1.2 Mb away from *bhP42 (www.wormbase.org)*.

Molecular biology

All PCR and sequencing primers are listed in Supplementary Table 1. The *pry-1(mu38) ayIs4; lin-12(n676n909), pry-1(mu38); lip-1 (zh15),* and *pop-1(hu9); muIs32; lin-12(n952)* strains were confirmed by sequencing *lin-12* (primers GL477/GL478), *lip-1* (GL466/GL467/GL468), and *pop-1* (GL508/GL509) mutations, respectively (Berset et al., 2001; Greenwald and Seydoux, 1990; Korswagen et al., 2002).

The *Cbr-pry-1* locus was PCR amplified in two large fragments (excluding intron 7) using primers GL104, GL106 (3.6 kb) and GL107, GL105 (2.2 kb). No mutation was detected in any of the exons or exon-intron junctions in *sy5270* animals suggesting that the mutation may be located in a non-coding regulatory region. In the case of *sy5353* there is a G to A transition at the first base of intron 6 that is predicted to disrupt the splicing donor site. There are two in frame stop codons (TAA and TGA) within 40 bp. The *sy5411* allele carries a GC insertion in exon 5 (+1761 from translational start site, flanking sequences TCGGCGCGC and CAGCCGTAC) that is expected to alter the reading frame leading to the introduction of two premature in frame stop codons (TGA and TAA) within 125 bp. All mutations were confirmed by sequencing both strands.

To construct *Cbr-pry-1::GFP*, 3.6 kb and 5 kb 5' UTR fragments were amplified by PCR using primers GL306/GL218 and GL217/GL218, respectively. The PCR products were digested (*Sph*I and *Sal*I for 3.6 kb, *Pst*I and *Sal*I for 5 kb) and subcloned into pPD95.69 (Fire lab vector, *www.addgene.com*). The *daf-6::YFP* construct was made by subcloning a 3 kb *Pst*I, *Kpn*I digested 5' UTR fragment (amplified by PCR using primers GL176/GL177) into pPD136.61.

All RNAi constructs were made by subcloning PCR products into *Sac*I, *Kpn*I digested double-T7 RNAi vector L4440 (Fire Lab vector kit, *www.addgene.com*). The DNA fragments are as follows: 0.9 kb genomic fragment of *Cbr-sys-1* (primers GL311/GL312), 2.3 kb genomic fragment of *Cbr-pop-1* (GL184/GL185), 2.4 kb genomic fragment of *Cbr-lin-39* (GL313/GL314), and 1.5 kb genomic fragment of *Cbr-lip-1* (GL464/GL465). The heat-shock promoter (hsp16-41) driven *Cbr-pry-1* construct was made by subcloning the full-length *Cbr-pry-1* cDNA into the Fire lab pPD49.83 vector.

RNAi

Since the wild type *C. briggsae* (AF16) is resistant to environmental RNAi, we used a transgenic strain *mfIs42* that carries wild type copy of the *C. elegans sid-2* gene. *mfIs42* animals are sensitive to environmental RNAi similar to the wild-type *C. elegans* (Winston et al., 2007). RNAi was performed on plates containing 0.6% Na_2HPO_4, 0.3% KH_2PO_4, 0.1% NH_4Cl, 0.5% Casamino Acids, 2% Agar, 1 mM $CaCl_2$, 1 mM $MgSO_4$, 0.0005% cholesterol, 0.2% β-lactose, and 50 μg/ml Carbenicillin. Plates were seeded with 100 μl of overnight grown HT115 bacterial culture in LB and Carbenicillin media that produces dsRNA of the gene of interest. Three to 5 L4 stage worms were placed on RNAi plates and the phenotypes of F1 progeny were examined. For genes that caused sterility and early stage lethality, animals were subjected to RNAi treatment during L1 larval stage. All RNAi experiments were repeated 3-4 times and batches that produced consistent results were analyzed.

The *C. briggsae* genome contains two *lin-12*-like genes one of which appears to be a *Cbr-lin-12* paralog (99% sequence identity) *(www.wormbase.org)*. The *Cbr-lin-12* RNAi construct used in this study is expected to inactivate both copies. This construct was described earlier and used to study *lin-12* function in *C. briggsae* (Felix, 2007). The amplified genomic region lacks significant sequence similarity to *Cbr-glp-1*, a *Cbr-lin-12/Notch* family member, ruling out the possibility of an RNAi off-target effect. Furthermore, the *Cbr-lin-12 and Cbr-glp-1* RNAi phenotypes are different and can be easily distinguished (Rudel and Kimble, 2001; Rudel and Kimble, 2002) (BPG, unpublished). Hence the *Cbr-lin-12* RNAi results described below are likely to be specific to *Cbr-lin-12* and its paralog.

Results

Isolation and molecular characterization of C. briggsae pry-1

To identify genes involved in vulval development in *C. briggsae*, we carried out EMS mutagenesis screens and isolated mutants that exhibit ectopic vulval induction leading to the formation of multiple pseudo-vulvae in adults. Out of 10 such mutants that were recovered from the screen, three (*sy5270, sy5353*, and *sy5411*) failed to complement (Table 1) and defined a locus on chromosome 1. All three alleles showed high frequency of ectopically induced VPCs (Table 1). In many cases (40%; n = 25 for *sy5353*) the migration of gonad arms was also defective. The males also showed abnormal tail morphologies such as ectopic anterior rays, crumpled spicules and pseudovulvae-like structures (data not shown).

To understand the mechanism of *sy5353* function in vulval development, we determined the molecular identity of the locus. A combination of phenotypic markers, polymorphism-based mapping,

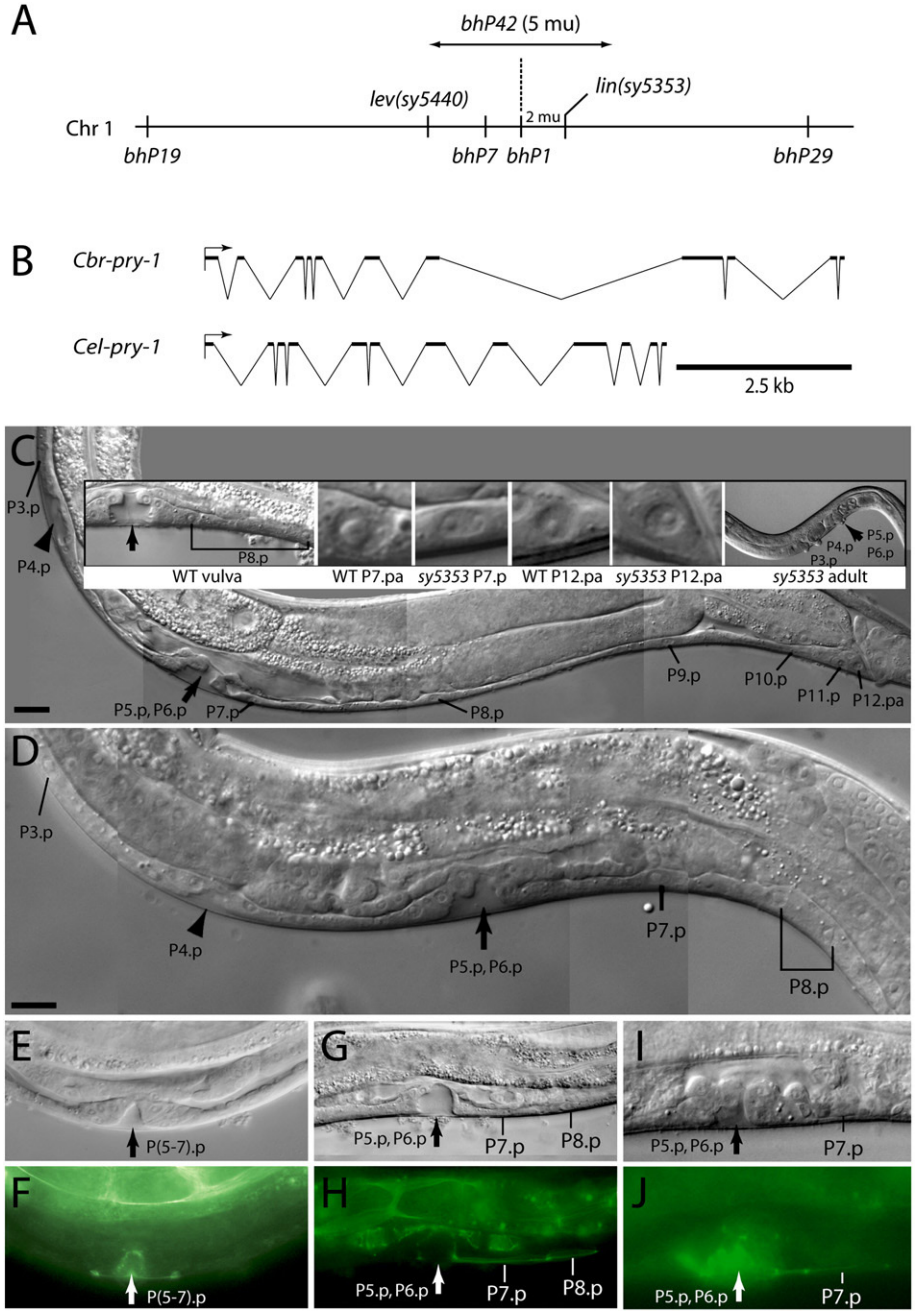

Fig. 1. (A) The locations of various markers and *lin(sy5353)* on chromosome 1. The *sy5353* mutation is tightly linked to indels *bhP7, bhP1* and *bhP42*. (B) The open reading frames (ORFs) of *pry-1* in *C. briggsae* and *C. elegans*. Major differences between the two ORFs include one less exon and two larger introns towards the 3' end in *C. briggsae* compared to *C. elegans*. (C-J) Vulval induction defect in *pry-1* mutants. Thick arrows mark the main vulva whereas arrowheads mark ectopic vulval invaginations. (C) The posterior VPCs are uninduced in a *sy5353* animal. The inset panels show a wild-type (WT) vulva and the nuclei of P7.p, P7.pa and P12.pa in WT and *sy5353* animals, and a *sy5353* adult showing anterior pseudovulvae. (D) A *pry-1(mu38)* animal showing induced P4.p and uninduced P7.p. (E-J) Analysis of the cell fusion defect using *dlg-1::GFP (mfEx33)* in *Cbr-pry-1(sy5353)* and *ajm-1::GFP (dels4)* in *pry-1(mu38)*. Unlike the wild type (E, F) where the progeny of P(5-7).p fuse to form seven concentric toroids, in the *sy5353* animal (G, H) P7.p and P8.p precursors remain unfused. (I, J) An unfused P7.p in *pry-1(mu38)* revealed by *ajm-1::GFP* expression. Anterior is to the left in all cases. The scale bars in C (same for E-J, except inset in C) and D are 10 μm.

and *C. briggsae* genome sequence assembly (Hillier et al., 2007) enabled us to take a candidate gene approach. A search for the *C. elegans* orthologs in the vicinity of linked polymorphisms *bhP1, bhP7* and *bhP42* (Fig. 1A and Supplementary Fig. 1) revealed a Wnt pathway component *pry-1* (*Axin* family) that is known to negatively regulate vulval induction (Gleason et al., 2002). The results of the following experiments indicate that *sy5353* is an allele of *C. briggsae pry-1*. First, we found that the RNAi-mediated knockdown of *Cbr-pry-1* phenocopies *sy5353* (Table 1). Second, overexpression of *Cbr-pry-1* full-length cDNA (using *hsp16-41* heat-shock promoter, *hsp::Cbr-pry-1*) rescues the mutant phenotype in more than half of the *sy5353* animals (53% wild type, n = 163, compared to 3% wild type, n = 39 in *sy5353* animals without heat shock). Finally, we sequenced *Cbr-pry-1* alleles and identified *sy5353* and *sy5411* mutations that introduce premature in-frame stop codons (see Materials and Methods and Supplementary Fig. 2), suggesting that both are likely to be *Cbr-pry-1* hypomorphs.

A comparison of the *pry-1* genomic regions between *C. elegans* and *C. briggsae* revealed the absence of one exon, as well as comparatively larger sizes for two introns in *C. briggsae* (Fig. 1B). We aligned protein sequences of Axin family members in nematodes and vertebrates to

Table 1
Vulval induction analysis in mutant and RNAi-treated animals.

Genotype	RNAi target	% Induced VPCs						% Overinduced	Average VPC induction	n
		P3.p	P4.p	P5.p	P6.p	P7.p	P8.p			
+	-	0	0	100	100	100	0	0	3.0	50
Cbr-pry-1(sy5353)	-	39	82	100	100	17	21	93	3.7 +/- 0.9	44
Cbr-pry-1(sy5411)	-	76	86	98	100	2	12	95	3.7 +/- 0.7	43
Cbr-pry-1(sy5270)	-	53	47	100	100	77	32	86	4.1 +/- 1.1	50
Cbr-pry-1(sy5270/sy5353)	-	58	68	100	100	11	32	nd	nd	47
Cbr-pry-1(sy5270/sy5411)	-	54	74	100	100	4	36	nd	nd	50
+	-	X	X	X	X	100	57	na	na	7
Cbr-pry-1(sy5353)	-	X	X	X	X	0	0	na	na	8
mfIs42	-	0	0	100	100	100	0	0	3.0	100
mfIs42	*Cbr-pry-1*	2	3	100	100	98	2	6	3.1 +/- 0.3	90
Cbr-pry-1(sy5353); mfIs42	-	58	86	100	100	38	20	98	3.8 +/- 0.9	50
mfIs42	*Cbr-sys-1*	0	0	100	100	100	0	0	3.0	27
Cbr-pry-1(sy5353); mfIs42	*Cbr-sys-1*	78	70	100	100	59	22	82 (P=0.2225)	4.2 +/- 1.2 (P=0.1628)	27
mfIs42	*Cbr-bar-1*	0	0	100	100	100	0	0	3.0	30
Cbr-pry-1(sy5353); mfIs42	*Cbr-bar-1*	26	26	100	100	86	17	49 (P<0.0001)	3.4 +/- 0.8 (P=0.0799)	35
mfIs42	*Cbr-pop-1*	0	0	5	5	5	0	0	0.2 +/- 0.7	77
Cbr-pry-1(sy5353); mfIs42	*Cbr-pop-1*	12	22	78	83	54	12	31 (P<0.0001)	2.6 +/- 1.4 (P<0.0001)	59
mfIs42	*Cbr-mab-5*	0	0	100	100	100	0	0	3.0	100
Cbr-pry-1(sy5353); mfIs42	*Cbr-mab-5*	33	67	97	100	41	36	96 (P=0.8340)	3.8 +/- 0.8 (P=0.8159)	70
mfIs42	*Cbr-lin-39*	0	0	10	55	24	0	0	0.9 +/- 0.9	29
Cbr-pry-1(sy5353); mfIs42	*Cbr-lin-39*	7	4	30	89	15	0	7 (P<0.0001)	1.4 +/- 1.1 (P<0.0001)	27
mfIs42	*Cbr-lin-12*	0	5	100	100	100	0	5	3.1 +/- 0.2	44
Cbr-pry-1(sy5353); mfIs42	*Cbr-lin-12*	66	83	100	100	83	22	95 (P=0.8176)	4.5 +/- 1.0 (P<0.0022)	41
mfIs42	*Cbr-lip-1*	0	0	100	100	100	0	0	3.0	25
Cbr-pry-1(sy5353); mfIs42	*Cbr-lip-1*	60	55	100	100	71	19	88 (P=0.3683)	3.4 +/- 0.6 (P=0.097)	58
+	-	0	0	100	100	100	0	0	3.0	30
pry-1(mu38)	-	24	6	100	100	82	10	31	3.2 +/- 0.6	89
*pop-1(hu9)**	-	0	0	100	100	100	0	0	3.0	38
pop-1(hu9) pry-1(mu38)	-	0	0	100	100	97	0	0	3.0 +/- 0.2	31
+	*lin-12*	0	0	100	100	100	0	0	3.0	50
pry-1(mu38)	*lin-12*	38	13	100	100	85	8	49 (P=0.5364)	3.4 +/- 0.7 (P=0.2209)	53
+	*lip-1*	0	0	100	100	100	0	0	3.0	100
pry-1(mu38)	*lip-1*	16	7	100	100	98	4	28 (P=0.7305)	3.1 +/- 0.3 (P=1.0000)	57
lip-1(zh15)	-	0	0	100	100	100	0	0	3.0	30
pry-1(mu38); lip-1(zh15)#	-	65	47	100	100	96	68	92 (P<0.0001)	4.0 +/- 0.5 (P<0.0001)	77
lin-12(n952)	-	27	73	84	97	81	81	92	4.4 +/- 1.1	37
lin-12(n952)	*pop-1*	5	25	100	90	100	80	70 (P=0.1691)	3.9 +/- 1.0 (P=0.08)	20
*pop-1(hu9); lin-12(n952)**	-	0	31	88	100	100	94	100	3.8 +/- 0.5 (P=0.0107)	16
+	*lin-39*	0	0	55	55	73	0	0	1.8 +/- 0.8	22
lin-12(n952)	*lin-39*	0	13	30	39	39	9	9 (P<0.0001)	1.2 +/- 1.4 (P<0.0001)	23

'+' refers to wild-type genetic background (*C. briggsae* AF16 and *C. elegans* N2). 'X' denotes Pn.p cells that were ablated during the L2 stage. *Strains carry *mec-7::GFP (muls32)*. #Strain carries *egl-17::GFP (ayIs4)*. VPC: vulva precursor cell, n: number of animals examined, nd: not done, na: not applicable.

identify domains in *Cbr*-PRY-1 that may facilitate homodimerization and interactions with *C. briggsae* homologs of APC, GSK-3β and β-Catenin (Behrens et al., 1998; Ikeda et al., 1998; Luo et al., 2005; Schwarz-Romond et al., 2007) (Supplementary Fig. 3). The *C. briggsae* PRY-1 is 70% identical to its counterpart in *C. elegans* with various domains being 70-85% conserved (Supplementary Fig. 4). This level of identity is close to APR-1 (APC homolog; 77% identical) but much lower than GSK-3 (GSK-3β homolog; 95% identical).

pry-1 mutants exhibit both Overinduced and Underinduced phenotypes

The *Cbr-pry-1* alleles were isolated based on the presence of ectopic pseudo-vulvae in adults. The analysis of vulval phenotype in mid-L4 stage animals showed a unique defect in VPC induction pattern. Specifically, P3.p, P4.p, and P8.p were ectopically induced in most animals whereas P7.p remained uninduced (Table 1) (see Materials and Methods). The P5.p and P6.p fates were unaffected. We also looked at the placement of AC in such animals and found that it was always located on the top of P6.p and its descendents (data not shown). Frequently individual animals exhibited both Overinduced and Underinduced phenotypes (Fig. 1C). A similar, albeit less penetrant, defect was also observed in *C. elegans pry-1* mutants (Fig. 1D, Table 1). In some cases only P5.p and P6.p were induced, a phenotype that has previously been reported in *C. elegans* (Gleason et al., 2002). The vulval cell lineages of mutant animals further supported these findings (Table 2). Thus, *pry-1* appears to play a similar role in both species.

A careful examination of Pn.p cells in *Cbr-pry-1* mutants revealed an additional defect in that all P(7-11).p cell nuclei were significantly smaller in size compared to wild type, appearing similar to P12.pa (Fig. 1A inset). It remains to be determined whether such a morphological change is caused by transformation to P12.pa-like cell fate. This phenotype is distinct from *C. elegans pry-1(mu38)* which do not show an obvious change in the morphology of posterior Pn.p cells (except P11.p) (see P7.p in Fig. 1D, data not shown). Considering that mutations in *C. elegans* Wnt pathway genes cause cell fate transformation due to alterations in Hox gene expression (Korswagen et al., 2002; Maloof et al., 1999), it is tempting to speculate that similar changes may underlie the Pn.p transformation phenotype in *Cbr-pry-1* mutants.

We examined posterior VPCs in *pry-1* mutants using cell junction-associated markers *ajm-1* (in *C. elegans*) and *dlg-1* (in *C. briggsae*) that identify epithelial cell boundaries. The AJM-1 (novel coiled-coil protein) and DLG-1 (*Drosophila* Disc Large family) are localized to apical junctions and are required for maintaining the integrity and polarity of junctional subdomains (Bossinger et al., 2001; Firestein and Rongo, 2001; Koppen et al., 2001). The *GFP* reporters for these genes mark VPCs and their progeny that do not fuse to the hyp7 (see Figs. 1E,F for *dlg-1::GFP* expression) (Sharma-Kishore et al., 1999) (Marie-Anne Felix, personal communication), and remain competent to respond to patterning signals. We found that uninduced P7.p and

Table 2
Cell lineage analysis of *pry-1* mutants in *C. elegans* and *C. briggsae*.

Genotype	P3.p	P4.p	P5.p	P6.p	P7.p	P8.p	n
Wild type*	S/SS	SS	LLTN	TTTT	NTLL	SS	25#
pry-1(mu38)	SON	SS	LLTN	OOTL	SOL	NLL	1
	SS	SS	LLTN	TTTT	NTLL	SS	1
	LLON	SS	LLTN	TTTT	NTLL	SS	1
	S	SS	LLTN	TOOO	NTLL	SS	1
	SS	SS	LLON	OTOL	S	NNNN	1
	S	SS	LLON	TTTT	LDOO	S	1
Cbr-pry-1(sy5353)	S	SS	LLLN	TLOO	U	U	1
	SL	SS	LLLN	ONTO	U	U	1
	NNNN	SS	LLLN	TONN	U	NNNN	1
	LNN	LNNT	LLON	TOOT	NOLL	NN	1
	TNNO	LNNO	LLLN	OOTO	U	U	1
	LNND	NNNN	LLON	TTTT	NTLL	U	1
	ONS	LNNT	LLTN	OOTT	U	SS	1
	SS	SS	LLON	TOTO	U	DNL	1
Cbr-pry-1(sy5411)	SN	LLNN	LLTN	TTTT	UU	NN	1
	NOLL	NNOT	NNNN	TOOT	UU	NN	1
	NNNN	NNNN	NTON	TOTO	UU	U	1
Cbr-pry-1(sy5270)	SOO	LOO	LLON	OOOD	NTLL	SS	1
	NNON	LNNT	LLON	OTOL	U	ONNL	1
	OTNO	LONO	LLON	TTTT	NLLN	SS	1
	SS	SS	LLLN	OTTO	NOLL	SNN	1
	S	NNNO	LLLN	OOOO	U	NONO	1
	SS	SS	LLLN	OOOO	NN	SS	1
	LNNL	SNL	LLLN	OOTO	U	NODL	1

*Wild-type *C. elegans* (N2) and *C. briggsae* (AF16) animals. #In each case lineages were observed for 25 animals. S, cell fused with syncytium; T, transverse plane of cell division; L, longitudinal; O, oblique; D, division plane not observed; N, no cell division; U, unfused cells that did not divide and appeared morphologically similar to P12.pa; n, number of animals examined. The cells attached to cuticle are underlined. In all cases, anchor cell was located on the top of the P6.p progeny.

P8.p in *pry-1* mutants are frequently unfused (Figs. 1G-J), which indicates that their lack of proliferation may be due to other defects. We also observed some cases of unfused P(9-11).p in *pry-1* mutants, which is similar to that reported earlier (Myers and Greenwald, 2007). These results suggest that in addition to maintaining competence, Wnt signaling also plays an important role in promoting cell proliferation and differentiation.

To determine whether P7.p and P8.p induction in *pry-1* mutants is inhibited by some unknown signal from neighboring VPCs we carried out VPC isolation experiments in *C. briggsae*. For this P(3-6).p cells were ablated during the early L2 stage with P7.p and P8.p being left intact. In contrast to wild-type animals where isolated P7.p and P8.p always adopted induced fates, these VPCs in *Cbr-pry-1(sy5353)* animals failed to do so (Table 1). It is unclear whether a lack in competence is due to the inability of VPCs to respond to signals that promote vulval cell proliferation or the Pn.p cells adopted a non-vulval fate.

Cbr-pry-1 is expressed in vulval precursors and their progeny

The molecular cloning of *Cbr-pry-1* facilitated the analysis of its expression pattern during development. We designed transcriptional *GFP* reporter plasmids using the 5' upstream genomic region of *Cbr-pry-1* (3.6 kb and 5 kb) and generated transgenic lines in *C. briggsae*. The *Cbr-pry-1::GFP* was expressed throughout the development, a finding similar to the *C. elegans pry-1* (Korswagen et al., 2002). The earliest expression was observed in embryos in numerous hypodermal cells. During the larval stages, the majority of the expression was seen in neurons in the ventral hypodermal region (Figs. 2A-D). Between L2 and L3 stages *Cbr-pry-1::GFP* was expressed in all six VPCs (see Figs. 2A-D for subsets of Pn.p cells). There was no obvious difference in the level of GFP fluorescence among the VPCs. The expression continued to persist in the vulval progeny of L4 stage animals (Figs. 2E-H), suggesting that *Cbr-pry-1* may also play a role in differentiation and morphogenetic processes. This is consistent with the abnormal vulval morphology in *Cbr-pry-1* mutants (Figs. 1C,G).

Cbr-pry-1 interacts with Wnt pathway components and a nuclear target in C. briggsae

Given that *Cbr-pry-1* encodes an Axin-like protein and that Axins are bona fide components of the canonical Wnt signaling pathway, we tested the interaction of *Cbr-pry-1* with *C. briggsae* orthologs of *C. elegans* Wnt pathway genes in vulval cell proliferation. The *Cbr-sys-1 (β-catenin)* knock-down (by RNAi) had no significant effect on the *Cbr-pry-1(sy5353)* vulval phenotype (Table 1), although animals exhibited severe defects in gonad morphology and were frequently sterile (data not shown). However, a similar RNAi experiment involving another *β-Catenin*, *Cbr-bar-1*, strongly suppressed the Overinduced phenotype of *Cbr-pry-1(sy5353)* (Table 1), suggesting that *Cbr-bar-1* is likely to act genetically downstream of *Cbr-pry-1*. We also found that compared to control animals P7.p in *Cbr-pry-1(sy5353); Cbr-bar-1 (RNAi)* was significantly more induced ($p = 0.0002$, Table 1).

Next, we examined the role of the *tcf/lef* family member *Cbr-pop-1* in *Cbr-pry-1*-mediated vulval development. The RNAi-mediated knock-down of *Cbr-pop-1* suppressed ectopic VPC induction in *Cbr-pry-1(sy5353)* (54% induced, 10% P12.pa-like, 36% 3°, and no F fates, $n = 59$ animals compared to 38% induced, 62% P12.pa-like and no 3°, or F fates, $n = 50$ animals in control) (Table 1). Similar to *Cbr-bar-1* RNAi, we also found an increased number of induced P7.p in *Cbr-pry-1 (sy5353) Cbr-pop-1(RNAi)* animals (Table 1). Interestingly, *Cbr-pop-1 (RNAi)* animals alone showed severe defects in vulval cell proliferation (no P12.pa-like, 55% 3° and 29% F fates, $n = 25$) (Fig. 3A, Table 1), suggesting its essential role in regulating VPC competence and induction. Although no such defect was observed in *C. elegans pop-1 (RNAi)* and *pop-1(hu9)* (a viable hypomorph) animals, both strongly suppressed the *pry-1(mu38)* phenotype (Table 1 and data not shown). These results demonstrate that *bar-1-pop-1*-mediated canonical Wnt signaling plays a conserved role in vulval development in *C. elegans* and *C. briggsae*.

Studies in *C. elegans* have identified transcriptional targets of Wnt signaling that include Hox genes *lin-39 (Dfd/Scr* family) and *mab-5* (*Antp* Hox family) (Eisenmann, 2005). *lin-39* is required at multiple times in vulval cells. During the L2 stage, *lin-39*-mediated canonical Wnt signaling prevents VPCs from fusing to the hyp7 syncytium (Eisenmann et al., 1998). Later on, during the L3 stage, *lin-39* is involved in the specification of VPC fates (Eisenmann, 2005). Unlike *lin-39*, *mab-5* appears to play a limited role in vulval development. *mab-5* is expressed in P7.p and P8.p and regulates the responsiveness of these two cells to inductive signal (Clandinin et al., 1997; Salser et al., 1993). We found that the RNAi-mediated knock-down of *Cbr-mab-5* had no effect on VPC induction in either wild type or *Cbr-pry-1(sy5353)* animals (Table 1). By contrast *Cbr-lin-39* RNAi caused abnormal vulval morphology due to cell fusion and cell fate specification defects (37% F and 33% 3° fates, respectively; $n = 46$ Pn.p cells) (Fig. 3B, Table 1). We also examined the *Cbr-pry-1 (sy5353); Cbr-lin-39(RNAi)* animals and found that of the 54% of P(3-8).p ($n = 28$) that were unfused in L2 (i.e., did not adopt an F fate), one-third fused to hyp7 in L3 (3° fate) whereas the remaining cells were induced giving rise to vulval progeny that invaginated during L4 stage. Overall, the RNAi-mediated knock-down of *Cbr-lin-39* strongly suppressed the Overinduced phenotype of *Cbr-pry-1(sy5353)* animals (Table 1). These results demonstrate that, similar to *C. elegans*, *Cbr-lin-39* acts downstream of *Cbr-pry-1* to regulate VPC competence and cell fate in *C. briggsae*.

Ectopically induced VPCs in pry-1 mutants acquire 2° fates

The ectopic induction of VPCs in *pry-1* mutants led us to examine cell fates using GFP-based markers. For this we made use of six different reporter genes in *C. elegans* (*syg-2* – immunoglobulin superfamily, *daf-6* – *patched*-related, *dhs-31* – short-chain dehydrogenase/reductase, *egl-17* – *fibroblast growth factor (fgf)* family, *lin-11* – LIM homeobox family, and *ceh-2* – *Drosophila empty spiracles (ems)*

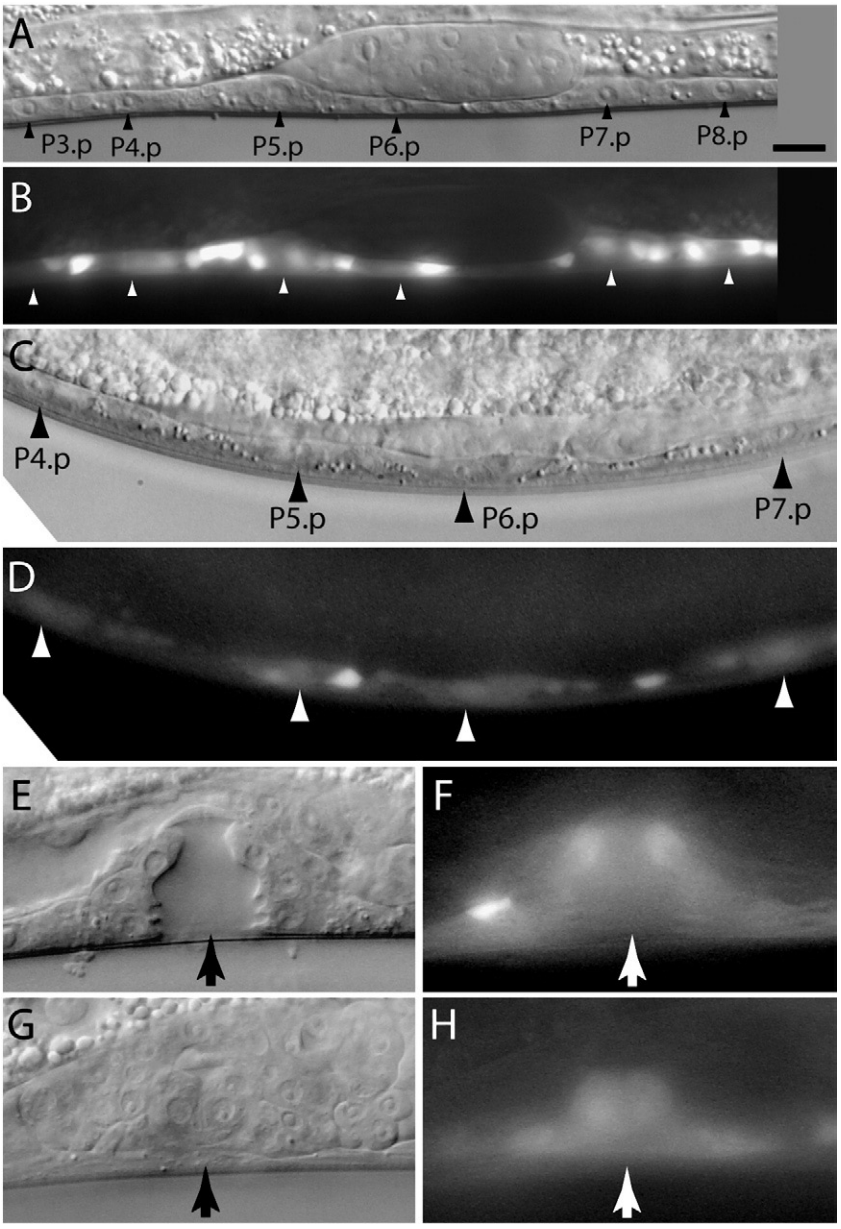

Fig. 2. *Cbr-pry-1::GFP* transcriptional reporter expression in *C. briggsae*. L2 stage *bhEx83* (A, B) and L3 stage *bhEx84* (C, D) transgenic animals showing GFP fluorescence in VPCs (arrowheads) and adjacent neuronal cells. Not all VPCs are visible in C and D. (E-H) *Cbr-pry-1::GFP* continues to be expressed in vulval progeny at later stages. GFP fluorescing cells viewed from two different focal planes in a mid-L4 stage *bhEx83* animal. The arrows mark the center of vulval invagination. Anterior is to the left in all cases. The scale bar in A is 10 μm.

homeodomain family) and two in *C. briggsae* (*Cbr-zmp-1* – zinc metalloproteinase family and *Cbr-egl-17*). These reporter genes are expressed in subsets of 1° and 2° lineage vulval cells and serve as faithful markers to assess induced VPC fates (Burdine et al., 1998; Felix, 2007; Gupta et al., 2003; Inoue et al., 2002; Perens and Shaham, 2005; Shen et al., 2004). In the case of *pry-1(mu38)* we found that four 2° lineage markers, namely *egl-17::GFP (ayIs4)*, *lin-11::GFP (syIs80)*, *ceh-2::GFP (syIs54)* (all mid/late-L4 stage) and *dhs-31::GFP (syIs101)* (old adult stage), were expressed in the progeny of all induced VPCs, P6.p excepted (Fig. 4A). Consistent with this, the expression of 1° lineage markers *egl-17::GFP (ayIs4)* (early/mid-L3 stage), *daf-6::YFP (bhEx53)* and *syg-2::GFP (wyEx3372)* (both mid/late-L4 stage) was localized to P6.p progeny (Fig. 4B). A similar phenotype was observed in *Cbr-pry-1(sy5353)* animals. Thus, *Cbr-egl-17::GFP* (*mfIs5*; a 2° lineage marker during mid-L4 stage) was expressed in the progeny of all induced VPCs, except P6.p, suggesting that these cells had

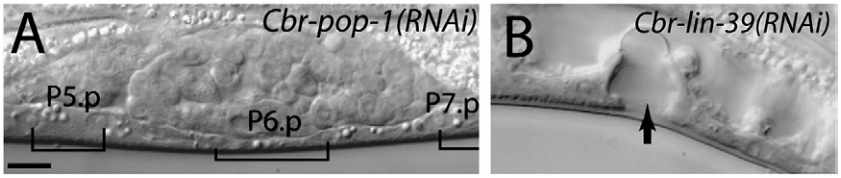

Fig. 3. Vulval induction defects in RNAi-treated animals. (A) *Cbr-pop-1(RNAi)*. P(5-7).p have adopted uninduced 3° fates. (B) Vulval invagination in a *Cbr-lin-39(RNAi)* animal formed by the progeny of P6.p. Other VPCs are uninduced. Anterior is to the left in both animals. The scale bar is 10 μm.

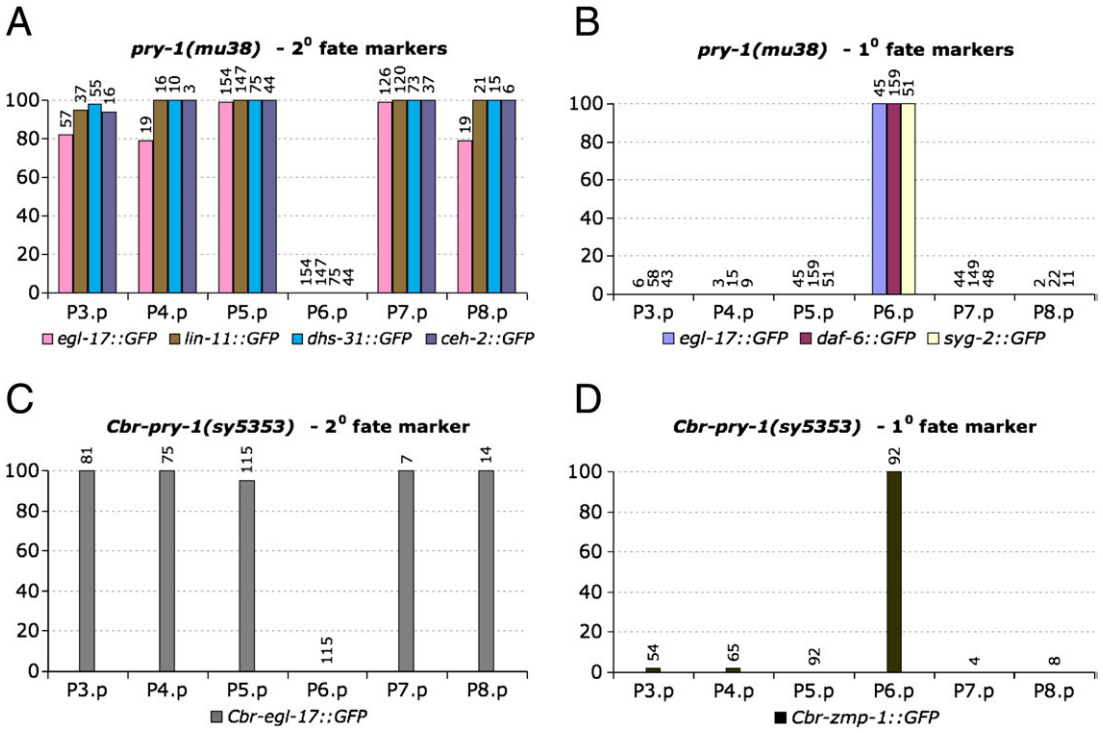

Fig. 4. Expression analysis of vulval cell fate markers in *pry-1* mutants. The y-axis represents the percentage of VPCs expressing the marker. The numbers above the bars show induced VPCs that were examined for GFP fluorescence. The 2° lineage markers are expressed in the progeny of all but P6.p whereas 1° lineage markers are expressed in P6.p progeny only. (A) 2° lineage markers in *C. elegans* – *egl-17::GFP (ayIs4)*, *lin-11::GFP (syIs80)*, *dhs-31::GFP (syIs101)*, and *ceh-2::GFP (syIs54)*. (B) 1° lineage markers in *C. elegans* – *egl-17::GFP (ayIs4)*, *daf-6::YFP (bhEx53)*, and *syg-2::GFP (wyEx3372)*. (C) 2° lineage marker *Cbr-egl-17::GFP (mfIs5)* in *C. briggsae*. (D) 1° lineage marker *Cbr-zmp-1::GFP (mfIs8)* in *C. briggsae*.

adopted 2° fates (Fig. 4C). In no case was *Cbr-egl-17::GFP* expression observed in P6.p progeny. This agrees with *Cbr-zmp-1::GFP* expression (*mfIs8*; a 1° lineage marker during late-L4 stage) that was restricted to P6.p progeny (Fig. 4D). Taken together, these results provide evidence that activated Wnt signaling confers 2° fate on VPCs in both species and that this mechanism is evolutionarily conserved.

VPCs in pry-1 mutants can adopt 2° fates in a gonad-independent manner

Previous studies have shown that the gonad plays an important role in vulval induction. The gonadal AC is a source of the LIN-3/EGF ligand that activates the LET-23/EGFR-mediated MPK-1/MAP kinase signaling pathway in VPCs leading to the specification of 1° and 2° fates (Sternberg, 2005). In addition, at least two Wnt genes (*mom-2* and *lin-44*) are expressed in several gonadal cells (Inoue et al., 2004), suggesting that the gonad may also be the source of a Wnt signal. For these reasons we assessed the contribution of the gonad to the *pry-1* phenotype by ablating gonad precursors in L1 stage. The examination of cell fates by 1° and 2° markers (*Cbr-zmp-1::GFP* and *Cbr-egl-17::GFP*, respectively) revealed that induced VPCs in gonad-ablated *Cbr-pry-1* mutants acquire a 2° fate (100%, n = 19 cells in 8 animals) (Fig. 5A,B; Table 3). In no case was a 1° fate observed in such ablated animals (n = 10 induced cells in 5 animals). Similar results were also obtained in *C. elegans pry-1(mu38)* animals using *egl-17::GFP* marker (57% 2° fate, n = 7 induced cells in 11 animals and no 1° fate, n = 5 induced cells in 6 animals) (Table 3). Thus, in both species Wnt signaling appears to be capable of conferring 2° fates independently of a gonad-derived signal.

VPCs in pry-1 mutants can adopt 2° fates in the absence of LIN-12/Notch signaling

Since the LIN-12/Notch-mediated lateral signaling pathway is required for 2° fate induction in *C. elegans* (Greenwald, 2005; Sternberg, 2005), we examined its role in *pry-1*-mediated VPC fate specification. Previous studies have shown that *Cbr-lin-12* is involved in *C. briggsae* vulval development (Felix, 2007; Rudel and Kimble, 2002). We took the RNAi approach to examine *Cbr-lin-12* interaction with *Cbr-pry-1* in vulval cells. Although the RNAi-mediated knock-down of *Cbr-lin-12* in control animals caused a subtle Overinduced phenotype due to rare ectopic induction of P4.p (5%, n = 44) (Table 1) and an abnormal vulval morphology (Fig. 5C), similar to that reported earlier (Felix, 2007) (also see Materials and Methods), it did not suppress ectopic vulval induction in *Cbr-pry-1(sy5353)* animals (Fig. 5D, Table 1).

Similar to *C. briggsae* the *lin-12* RNAi in *C. elegans* also had no effect on the *pry-1(mu38)* vulva phenotype (Table 1). We further examined the *lin-12*-independent role of *pry-1* using a null allele, *n676n909*. In *lin-12(n676n909)* animals, P5.p, P6.p, and P7.p each adopt a 1° fate (Greenwald et al., 1983), resulting in an abnormally large vulval protrusion (termed protruding vulva or Pvl) in adults. We generated *pry-1(mu38); lin-12(n676n909)* double mutant animals carrying *egl-17::GFP (ayIs4)* and found that such animals exhibit a combination of Overinduced and Pvl phenotypes (Fig. 5E) and show GFP fluorescence in ectopically induced VPCs (Fig. 5F). In these animals (n = 12) P5.p and P7.p were always induced but had no detectable level of GFP fluorescence. These results demonstrate that vulval development in *pry-1* mutants can occur in the absence of *lin-12* function and ectopically induced VPCs are capable of adopting a 2° fate.

We also examined the interaction of *pry-1* with *lip-1* (MAP kinase phosphatase), a transcriptional target of *lin-12*, that promotes 2° VPC fate by inhibiting MAP kinase activity and a 1° cell fate (Berset et al., 2001). The RNAi-mediated knock-down of *lip-1* in both *C. elegans* and *C. briggsae pry-1* mutants had no obvious effect on vulval induction except that P7.p was almost always induced (Table 1). The *lip-1* hypomorph (deletion allele *zh15*) also failed to suppress the *pry-1* Overinduced phenotype. On the contrary, we observed a significant increase in induced VPCs in *pry-1(mu38); lip-1(zh15)* double mutants compared to *pry-1(mu38)* (92% vs. 31%) (Table 1). In these animals 98% of ectopically induced VPCs (n = 140) adopted a 2° fate as judged by the expression of *egl-17::GFP (ayIs4)*.

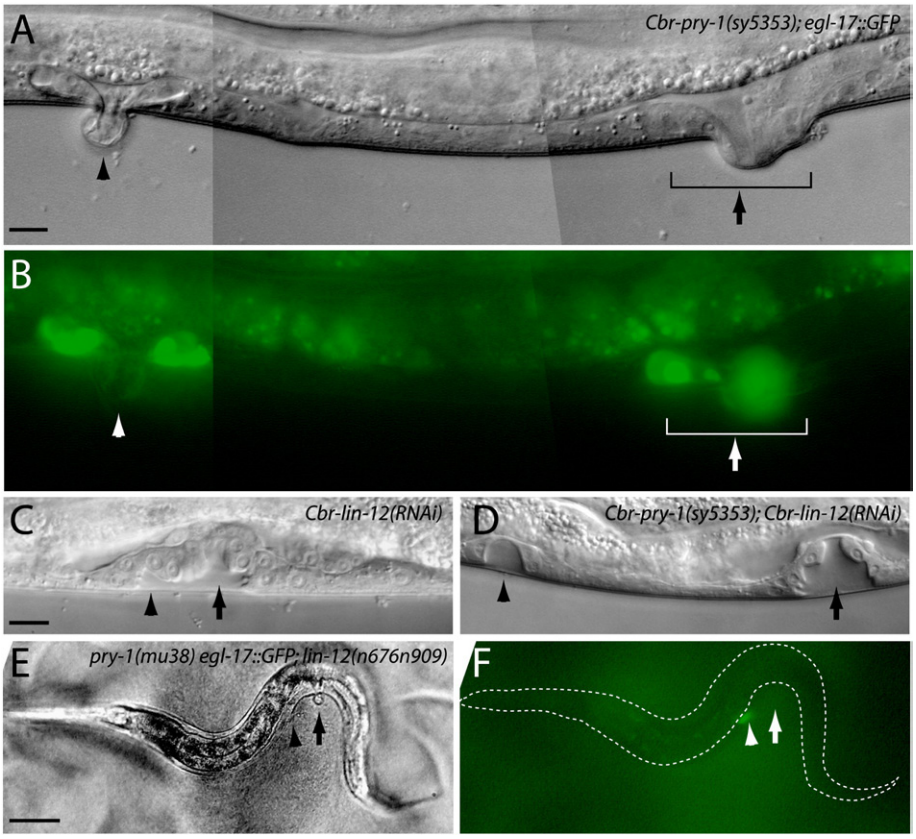

Fig. 5. Gonad-independent and *lin-12*-independent induction of VPCs in *pry-1* mutants. The ectopic vulval invagination and pseudo-vulvae are shown by arrowheads whereas main vulvae by arrows. (A, B) In this gonad-ablated *Cbr-pry-1(sy5353)* animal, *egl-17::GFP* expression can be observed in the progeny of P3.p, P5.p and P6.p. (C) A *Cbr-lin-12(RNAi)* animal showing ectopic induction of P4.p. (D) P7.p induction defect in *sy5353* is rescued by *Cbr-lin-12(RNAi)*. In this animal P4.p was also induced. (E, F) A *pry-1(mu38); lin-12(n676n909)* double mutant showing ectopic pseudovulva (due to induced P4.p) and protruding vulva phenotypes. The *egl-17::GFP* expression can be seen in the progeny of P4.p (arrowhead). Anterior is to the left in all cases. The scale bars are 10 μm (A-D) and 100 μm (E,F).

While the above results suggest that *pry-1* function does not depend upon LIN-12/Notch pathway activity in both *C. elegans* and *C. briggsae*, these data do not rule out the possibility that *lin-12* may act upstream of Wnt signaling to promote 2° fates. To address this possibility we performed experiments with a weak gain-of-function *C. elegans lin-12* allele *n952* that causes ectopic vulval induction in roughly two-thirds of animals (Table 1) (Greenwald et al., 1983). The incomplete penetrance of *lin-12(n952)* provides a sensitized genetic background to test the impact of alterations in Wnt pathway effectors *pop-1* and *lin-39* on vulval induction. We found that although *lin-39 (RNAi)* strongly suppressed *lin-12(n952)* vulval phenotype, *pop-1 (hu9)* and *pop-1(RNAi)* had no such effect (Table 1). These results suggest a simple model in which Wnt and LIN-12/Notch signaling pathways function independently via *lin-39* to specify 2° VPC fates in *C. elegans*.

Table 3
Induced VPCs in gonad-ablated *pry-1* mutants acquire 2° fates.

Genotype	Induced VPCs (Fraction of induced VPCs showing GFP fluorescence)						n
	P3.p	P4.p	P5.p	P6.p	P7.p	P8.p	
mfIs5	0	0	0	0	0	0	5
Cbr-pry-1(sy5353); mfIs5	4 (4/4)	3 (3/3)	4 (4/4)	8 (8/8)	0	0	8
ayIs4	0	0	0	0	0	0	5
ayIs4 pry-1(mu38)	0	3 (1/3)	0	1 (0/1)	2 (2/2)	1 (1/1)	11

n, number of animals examined.

Inhibition of lin-12/Notch signaling in pry-1 mutants promotes P7.p induction

Although the RNAi-mediated knock-down of *Cbr-lin-12* did not suppress ectopic vulval induction in *Cbr-pry-1(sy5353)* animals, we noted that it increased P7.p induction significantly ($P = 0.0003$, Table 1) and gave rise to a wild-type vulva in most animals (Fig. 5D). A similar trend was also observed in *pry-1(mu38); lin-12 (RNAi)* animals but the difference was statistically not significant (Table 1). This suggested that persistent activity of *lin-12/Notch* signaling in *pry-1* mutants might interfere with P7.p induction and cell fate specification. To examine this, we analyzed *lip-1* reporter expression that, in response to a *lin-12* signal, is upregulated in presumptive 2° VPCs in *C. elegans* (Berset et al., 2001). The expression of *lip-1::GFP* in *C. briggsae (mfIs29)* was first observed in all six VPCs during the L2 stage (50%, $n = 14$) (Figs. 6A,B). This pattern was dynamic, such that by the early/mid-L3 (Pn.p) stage the fluorescence could be seen in only P5.p and P7.p and was undetectable in other Pn.p cells (48%, $n = 21$) (Figs. 6C,D and data not shown). This indicates that while *lip-1* expression in *C. briggsae* is maintained in 2° precursors it is rapidly downregulated in 1° and other cells. An analogous pattern was observed in mid-L3 (Pn.px) stage animals although in few cases (27%, $n = 11$ animals) faint GFP fluorescence was also detected in P4.p and P8.p daughters. At later stages no fluorescence was seen in P(5-7).p progeny.

The analysis of *lip-1* reporter expression in *Cbr-pry-1(sy5353)* animals revealed a similar profile but the fluorescence was much higher in P7.p and P8.p cells. Thus, in L2 stage animals all six VPCs were seen fluorescing, with P7.p and P8.p being the brightest in half of the animals ($n = 6$) that showed GFP fluorescence (Figs. 6E,F). By the

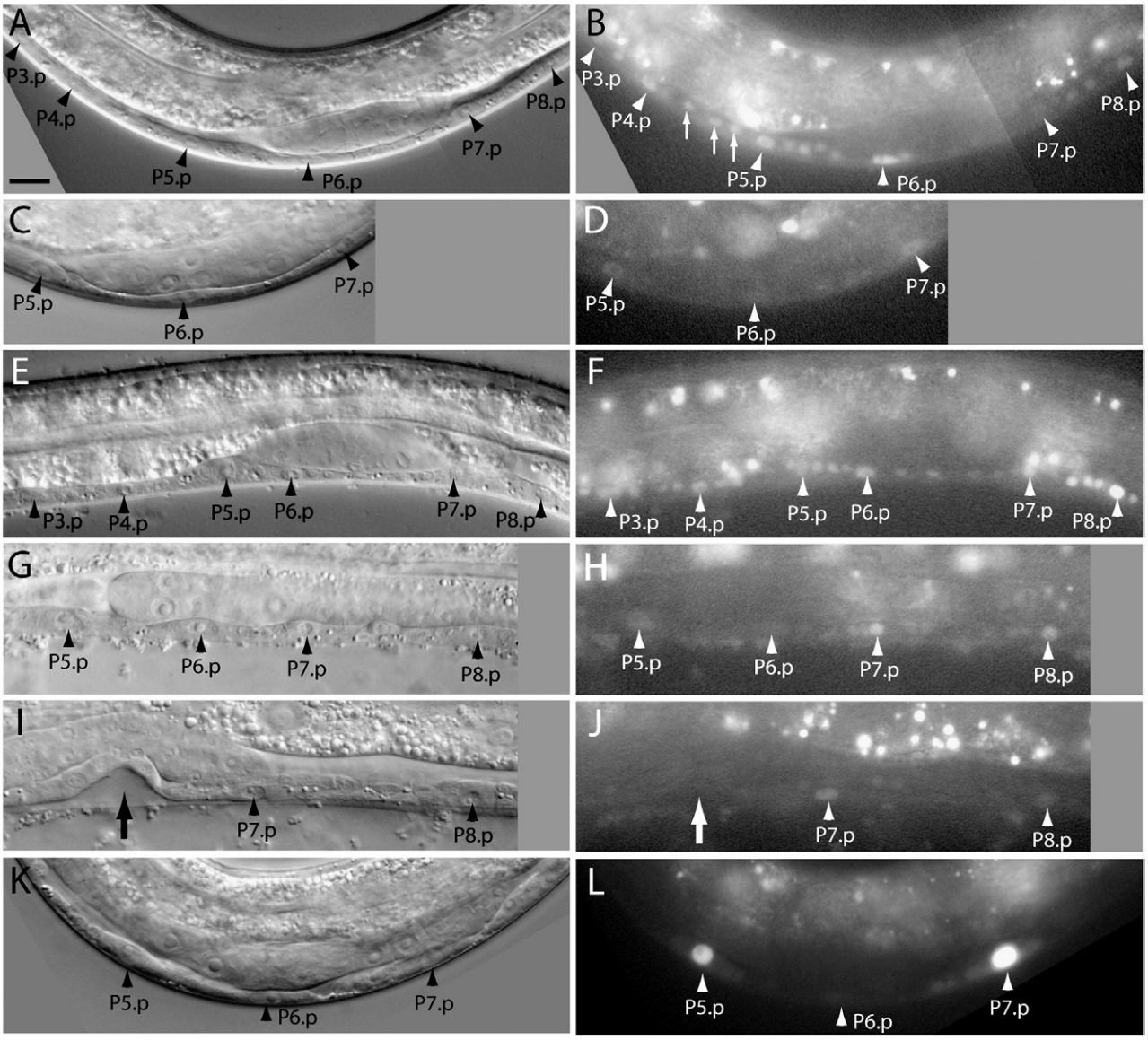

Fig. 6. *lip-1::GFP* expression patterns in wild type and *pry-1* mutants. Arrowheads point to VPCs whereas small arrows to some of the neuronal cells. The big arrows in panels I and J show vulval invagination formed by the progeny of P5.p and P6.p. (A-D) AF16; (E-J) *Cbr-pry-1(sy5353)*; (K, L) *pry-1(mu38)*. (A, B) The P(3-8).p VPCs and some of the neurons in this L2 stage animal can be seen fluorescing. (C, D) An early/mid-L3 stage animal showing GFP fluorescence in P5.p and P7.p. The fluorescence in P6.p is almost invisible. (E, F) P7.p and P8.p are fluorescing at a higher level in this L2 stage animal compared to other Pn.p cells. (G-J) The same two precursors continue to fluoresce at early/mid-L3 (G, H), and early-L4 (I, J) stages. (K, L) P7.p is fluorescing brightly compared to the P5.p. Anterior is to the left in all cases. The scale bar is 10 μm.

early/mid-L3 (Pn.p) stage, fluorescence had rapidly faded in P6.p and other anterior VPCs, however, P7.p and P8.p continued to fluoresce brightly (90%, n = 11 *GFP* expressing animals) (Figs. 6G,H). After the mid-L3 (Pn.px) stage, other than P7.p and P8.p, no VPC progeny showed detectable level of fluorescence (71%, n = 14 *GFP* expressing animals) (Figs. 6I,J). Similar to *C. briggsae* we found that *lip-1::GFP* expression in *C. elegans pry-1(mu38)* L2 stage animals was also higher in P7.p compared to anterior VPCs (37%, n = 19 *GFP* expressing animals) (Figs. 6K,L). These results show an abnormal pattern of *lip-1* expression in *pry-1* mutants and provide a molecular basis for P7.p induction defect in both species.

To further investigate genetic interaction between *lip-1* and *pry-1*, we examined P7.p phenotype in *pry-1* mutants by reducing *lip-1* activity. Consistent with our *lip-1* expression data, we found that RNAi-mediated knock-down of *Cbr-lip-1* in *Cbr-pry-1(sy5353)* animals caused a significant increase in P7.p induction (P = 0.0034) (Table 1). A similar, but weak, phenotype was also observed in *C. elegans pry-1(mu38); lip-1(RNAi)* and *pry-1(mu38); lip-1(zh15)* animals (P = 0.0163 and 0.1175, respectively) (Table 1). Furthermore, induced P7.p in *pry-1(mu38); lip-1(zh15)* animals showed *egl-17::GFP (ayIs4)* expression (100%, n = 60), suggesting that they adopted a 2° fate. Taken together, these findings provide evidence for a conserved interaction between Wnt and LIN-12/Notch signaling pathways to specify the 2° fate of P7.p in *C. elegans* and *C. briggsae*.

Discussion

Due to their apparent morphological similarity, *C. elegans* and *C. briggsae* offer unique advantages in comparative analysis of gene function and signaling networks. To study how homologous tissues are patterned in these two species, we are focusing on the vulva, a reproductive organ necessary for mating and egg laying. We carried out genetic screens in *C. briggsae* and isolated mutants that show defects in vulval development. In this study we report characterization of three of the mutants that exhibit an Overinduced phenotype and show that they are alleles of *Cbr-pry-1*. Our genetic experiments

have revealed that *Cbr-pry-1* functions in *Cbr-bar-1-Cbr-pop-1*-mediated canonical Wnt signaling pathway to regulate VPC induction and fate specification. We have also identified *Cbr-lin-39* Hox gene as a downstream target of this pathway. These findings demonstrate that, similar to *C. elegans*, canonical Wnt signaling pathway is involved in *C. briggsae* vulva formation. Both over- and under-activation of Wnt signaling causes vulval abnormalities thereby highlighting its key role in development. A recent study has shown that changes in environmental conditions have significant effects on Wnt signaling-mediated vulval induction (Braendle and Felix, 2008). This serves to further demonstrate the physiological importance of this pathway in patterning the vulva.

Wnt signaling confers 2° fate on VPCs

Previous studies have demonstrated the essential role of Wnt signaling in maintaining VPC competence (Eisenmann et al., 1998; Myers and Greenwald, 2007). During the L2 stage *bar-1*-mediated Wnt signaling promotes *lin-39* activity in P(3-8).p and allows these cells to respond to patterning signals in the L3 stage. Our work has revealed that in addition to its role in VPC competence, Wnt signaling also promotes a specific cell fate in *C. elegans* and *C. briggsae*. Previous work by Gleason and colleagues (Gleason et al., 2002) showed that activated Wnt signaling causes excessive vulval cell proliferation. However it was unclear whether vulval progeny adopted a specific fate. Subsequently, Myers and Greenwald (Myers and Greenwald, 2007) argued that ectopic vulval progeny in *pry-1* mutants could arise from spurious cell divisions due to high *lin-39* levels. To address this issue we analyzed cell fates in *pry-1* mutants using established molecular markers. We found that induced VPCs, except P6.p, in *pry-1* mutants adopted a 2° fate as judged by a panel of 8 GFP-based markers (6 in *C. elegans* and 2 in *C. briggsae*). The use of wide range of reporters used in our assay (i.e., ligands, cell surface receptors, metalloproteases, and transcription factors) serves to demonstrate that Wnt signaling orchestrates expression of many important genes needed to confer a 2° fate. In these animals the P6.p fate remained unaltered. Further experiments revealed that 2° VPC fates are specified independently of the gonad-derived inductive signal since induced VPCs in gonad-ablated animals showed 2° marker expression similar to that seen in intact animals. These results significantly extend our understanding of *pry-1*-mediated Wnt signaling function in two nematode species and suggest that Wnt signaling plays both permissive role (in maintaining competence) and instructive role (in specifying cell fate) in vulval development.

The 2° fates of induced VPCs in *pry-1* mutants prompted us to examine the relationship between Wnt and LIN-12/Notch signaling in vulval development. We found that alterations in the activities of LIN-12/Notch pathway receptor *lin-12* and its transcriptional target *lip-1* did not suppress ectopic vulval induction defect in *pry-1* mutants. Thus, activated Wnt signaling in *C. elegans* and *C. briggsae* is sufficient to promote vulval development in the absence of lateral signaling. This raises the question of evolutionary roles of Wnt and LIN-12/Notch pathways in 2° fate specification. Perhaps the two pathways evolved as redundant mechanisms to robustly specify a 2° VPC fate. The completed genome sequences of *Elegans* group species (such as *C. remanei* and *C. brenneri*) provide opportunities to address such questions.

Wnt signaling and P7.p fate specification

Our work has uncovered novel roles of the Wnt signaling pathway in *C. elegans* and *C. briggsae* vulval development that involve both positive and negative regulation of cell fates. We found that P3.p, P4.p, and P8.p in *pry-1* mutants are frequently induced to adopt a 2° fate whereas P7.p remains largely uninduced. This is likely to be caused by activated Wnt signaling since RNAi knock-downs of *Cbr-bar-1* and *Cbr-pop-1* promoted P7.p induction in *Cbr-pry-1* mutants. Since LIN-12/Notch-mediated lateral signaling specifies the 2° fate of P7.p, we examined its role in mediating *pry-1* function. Our results showed that the expression of *lip-1* in *pry-1* mutants was significantly higher in P7.p compared to P5.p and persisted in L4 stage animals. This pattern differs from wild type where *lip-1* is dynamically regulated in P(5-7).p and is not observed beyond mid-L3 stage. This suggests that a failure to downregulate *lip-1* in *Cbr-pry-1* mutants may be the basis of the P7.p induction defect. Considering that LIP-1 is a MAP kinase phosphatase, one model is that the persistence of high level of LIP-1 activity in P7.p (directly or indirectly induced by Wnt signaling) abnormally antagonizes *mpk-1* (MAP kinase, Ras pathway component) function such that the Ras pathway response in P7.p falls below the minimum threshold needed to promote an induced fate. It is equally possible that misregulation of *lip-1* interferes with the expression of *lin-12* target genes that in turn causes P7.p to remain uninduced. Consistent with these possibilities, we found that lowering *lip-1* activity (either by directly targeting *lip-1* or its upstream activator *lin-12*) in *pry-1* mutants suppressed the P7.p induction defect.

While our results provide evidence for a genetic interaction between Wnt and LIN-12/Notch signaling pathways, more work is needed to understand the mechanism of interaction and its biological role in P7.p development. In this respect, reverse genetics and genomics approaches could prove valuable in dissecting the roles of Wnt and LIN-12/Notch pathway genes and their downstream targets. These studies may uncover the function of new genes thereby revealing their mechanism of function and signaling crosstalk. Ultimately, the findings will help understand how changes in gene expression and interactions are regulated to generate tissue morphology.

Acknowledgments

We are indebted to Marie-Anne Félix (Institut Jacques Monod) for generously providing some of the transgenic strains and RNAi bacterial clones. The genetic screen was carried in the laboratory of Paul Sternberg (Caltech). We thank Shahla Gharib for isolating *sy5270*, Bavithra Thillainathan for help in mapping *sy5353*, Kang Shen (Stanford University) for providing *syg-2::GFP (wyEx3372)* strain, and Zhongying Zhao (University of Washington, Seattle) for the *C. briggsae unc-119* deletion allele *st20000*. We also thank Nathan Farrar for helpful comments on the manuscript. Some of the strains were obtained from the *Caenorhabditis* Genetics Center. This work was supported by funds from the Natural Sciences and Engineering Research Council of Canada and Canada Research Chairs Program to BPG.

Appendix A. Supplementary data

Supplementary data associated with this article can be found, in the online version, at doi:10.1016/j.ydbio.2010.07.003.

References

Avery, L., Horvitz, H.R., 1987. A cell that dies during wild-type *C. elegans* development can function as a neuron in a *ced-3* mutant. Cell 51, 1071–1078.
Behrens, J., Jerchow, B.A., Wurtele, M., Grimm, J., Asbrand, C., Wirtz, R., Kuhl, M., Wedlich, D., Birchmeier, W., 1998. Functional interaction of an axin homolog, conductin, with beta-catenin, APC, and GSK3beta. Science 280, 596–599.
Berset, T., Hoier, E.F., Battu, G., Canevascini, S., Hajnal, A., 2001. Notch inhibition of RAS signaling through MAP kinase phosphatase LIP-1 during *C. elegans* vulval development. Science 291, 1055–1058.
Bossinger, O., Klebes, A., Segbert, C., Theres, C., Knust, E., 2001. Zonula adherens formation in *Caenorhabditis elegans* requires *dlg-1*, the homologue of the *Drosophila* gene *discs large*. Dev. Biol. 230, 29–42.
Braendle, C., Felix, M.A., 2008. Plasticity and errors of a robust developmental system in different environments. Dev. Cell 15, 714–724.
Bray, S.J., 2006. Notch signalling: a simple pathway becomes complex. Nat. Rev. Mol. Cell Biol. 7, 678–689.
Brenner, S., 1974. The genetics of *Caenorhabditis elegans*. Genetics 77, 71–94.

Burdine, R.D., Branda, C.S., Stern, M.J., 1998. EGL-17(FGF) expression coordinates the attraction of the migrating sex myoblasts with vulval induction in *C. elegans*. Development 125, 1083–1093.
Clandinin, T.R., Katz, W.S., Sternberg, P.W., 1997. Caenorhabditis elegans HOM-C genes regulate the response of vulval precursor cells to inductive signal. Dev. Biol. 182, 150–161.
Coudreuse, D.Y., Roel, G., Betist, M.C., Destree, O., Korswagen, H.C., 2006. Wnt gradient formation requires retromer function in Wnt-producing cells. Science 312, 921–924.
Cutter, A.D., 2008. Divergence times in *Caenorhabditis* and *Drosophila* inferred from direct estimates of the neutral mutation rate. Mol. Biol. Evol. 25, 778–786.
Eisenmann, D. M., 2005. Wnt signaling. WormBook. ed. The *C. elegans* Research Community, WormBook. doi:10.1895/wormbook.1.7.1, http://www.wormbook.org.
Eisenmann, D.M., Kim, S.K., 2000. Protruding vulva mutants identify novel loci and Wnt signaling factors that function during Caenorhabditis elegans vulva development. Genetics 156, 1097–1116.
Eisenmann, D.M., Maloof, J.N., Simske, J.S., Kenyon, C., Kim, S.K., 1998. The beta-catenin homolog BAR-1 and LET-60 Ras coordinately regulate the Hox gene *lin-39* during *Caenorhabditis elegans* vulval development. Development 125, 3667–3680.
Eizinger, A., Sommer, R.J., 1997. The homeotic gene *lin-39* and the evolution of nematode epidermal cell fates. Science 278, 452–455.
Felix, M.A., 2005. An inversion in the wiring of an intercellular signal: evolution of Wnt signaling in the nematode vulva. Bioessays 27, 765–769.
Felix, M.A., 2007. Cryptic quantitative evolution of the vulva intercellular signaling network in *Caenorhabditis*. Curr. Biol. 17, 103–114.
Firestein, B.L., Rongo, C., 2001. DLG-1 is a MAGUK similar to SAP97 and is required for adherens junction formation. Mol. Biol. Cell 12, 3465–3475.
Gleason, J.E., Korswagen, H.C., Eisenmann, D.M., 2002. Activation of Wnt signaling bypasses the requirement for RTK/Ras signaling during *C. elegans* vulval induction. Genes Dev. 16, 1281–1290.
Gleason, J.E., Szyleyko, E.A., Eisenmann, D.M., 2006. Multiple redundant Wnt signaling components function in two processes during *C. elegans* vulval development. Dev. Biol. 298, 442–457.
Greenwald, I., 2005. LIN-12/Notch signaling in *C. elegans*. WormBook. ed. The *C. elegans* Research Community, WormBook. doi:10.1895/wormbook.1.10.1, http://www.wormbook.org.
Greenwald, I., Seydoux, G., 1990. Analysis of gain-of-function mutations of the *lin-12* gene of *Caenorhabditis elegans*. Nature 346, 197–199.
Greenwald, I.S., Sternberg, P.W., Horvitz, H.R., 1983. The *lin-12* locus specifies cell fates in *Caenorhabditis elegans*. Cell 34, 435–444.
Gupta, B. P., Johnsen, R., Chen, N., 2007. Genomics and biology of the nematode *Caenorhabditis briggsae*. WormBook. ed. The *C. elegans* Research Community, WormBook. doi:10.1895/wormbook.1.136.1, http://www.wormbook.org.
Gupta, B.P., Wang, M., Sternberg, P.W., 2003. The *C. elegans* LIM homeobox gene *lin-11* specifies multiple cell fates during vulval development. Development 130, 2589–2601.
Hall, D.H., Altun, Z.F., 2008. *C. elegans* Atlas. Cold Spring Harbor Laboratory Press, New York.
Herman, M.A., Vassilieva, L.L., Horvitz, H.R., Shaw, J.E., Herman, R.K., 1995. The *C. elegans* gene *lin-44*, which controls the polarity of certain asymmetric cell divisions, encodes a Wnt protein and acts cell nonautonomously. Cell 83, 101–110.
Hillier, L.W., Miller, R.D., Baird, S.E., Chinwalla, A., Fulton, L.A., Koboldt, D.C., Waterston, R.H., 2007. Comparison of *C. elegans* and *C. briggsae* Genome Sequences Reveals Extensive Conservation of Chromosome Organization and Synteny. PLoS Biol. 5, e167.
Ikeda, S., Kishida, S., Yamamoto, H., Murai, H., Koyama, S., Kikuchi, A., 1998. Axin, a negative regulator of the Wnt signaling pathway, forms a complex with GSK-3beta and beta-catenin and promotes GSK-3beta-dependent phosphorylation of beta-catenin. EMBO J. 17, 1371–1384.
Inoue, T., Oz, H.S., Wiland, D., Gharib, S., Deshpande, R., Hill, R.J., Katz, W.S., Sternberg, P.W., 2004. *C. elegans* LIN-18 is a Ryk ortholog and functions in parallel to LIN-17/Frizzled in Wnt signaling. Cell 118, 795–806.
Inoue, T., Sherwood, D.R., Aspock, G., Butler, J.A., Gupta, B.P., Kirouac, M., Wang, M., Lee, P.Y., Kramer, J.M., Hope, I., Burglin, T.R., Sternberg, P.W., 2002. Gene expression markers for *Caenorhabditis elegans* vulval cells. Mech. Dev. 119 (Suppl 1), S203–S209.
Kenyon, C.J., Austin, J., Costa, M., Cowing, D.W., Harris, J.M., Honigberg, L., Hunter, C.P., Maloof, J.N., Muller-Immergluck, M.M., Salser, S.J., Waring, D.A., Wang, B.B., Wrischnik, L.A., 1997. The dance of the Hox genes: patterning the anteroposterior body axis of *Caenorhabditis elegans*. Cold Spring Harb. Symp. Quant. Biol. 62, 293–305.
Koboldt, D.C., Staisch, J., Thillainathan, B., Haines, K., Baird, S.E., Chamberlin, H.M., Haag, E.S., Miller, R.D., Gupta, B.P., 2010. A toolkit for rapid gene mapping in the nematode Caenorhabditis briggsae. BMC Genomics 11, 236.
Koppen, M., Simske, J.S., Sims, P.A., Firestein, B.L., Hall, D.H., Radice, A.D., Rongo, C., Hardin, J.D., 2001. Cooperative regulation of AJM-1 controls junctional integrity in *Caenorhabditis elegans* epithelia. Nat. Cell Biol. 3, 983–991.
Korswagen, H.C., Coudreuse, D.Y., Betist, M.C., van de Water, S., Zivkovic, D., Clevers, H.C., 2002. The Axin-like protein PRY-1 is a negative regulator of a canonical Wnt pathway in *C. elegans*. Genes Dev. 16, 1291–1302.
Logan, C.Y., Nusse, R., 2004. The Wnt signaling pathway in development and disease. Annu. Rev. Cell Dev. Biol. 20, 781–810.
Louvet-Vallee, S., Kolotuev, I., Podbilewicz, B., Felix, M.A., 2003. Control of vulval competence and centering in the nematode *Oscheius* sp. 1 CEW1. Genetics 163, 133–146.
Luo, W., Zou, H., Jin, L., Lin, S., Li, Q., Ye, Z., Rui, H., Lin, S.C., 2005. Axin contains three separable domains that confer intramolecular, homodimeric, and heterodimeric interactions involved in distinct functions. J. Biol. Chem. 280, 5054–5060.
Maduro, M., Pilgrim, D., 1995. Identification and cloning of *unc-119*, a gene expressed in the *Caenorhabditis elegans* nervous system. Genetics 141, 977–988.
Maloof, J.N., Whangbo, J., Harris, J.M., Jongeward, G.D., Kenyon, C., 1999. A Wnt signaling pathway controls hox gene expression and neuroblast migration in C. elegans. Development 126, 37–49.
Mello, C.C., Kramer, J.M., Stinchcomb, D., Ambros, V., 1991. Efficient gene transfer in *C. elegans*: extrachromosomal maintenance and integration of transforming sequences. EMBO J. 10, 3959–3970.
Myers, T.R., Greenwald, I., 2007. Wnt signal from multiple tissues and *lin-3*/EGF signal from the gonad maintain vulval precursor cell competence in *Caenorhabditis elegans*. Proc. Natl Acad. Sci. USA 104, 20368–20373.
Perens, E.A., Shaham, S., 2005. *C. elegans daf-6* encodes a patched-related protein required for lumen formation. Dev. Cell 8, 893–906.
Rocheleau, C.E., Downs, W.D., Lin, R., Wittmann, C., Bei, Y., Cha, Y.H., Ali, M., Priess, J.R., Mello, C.C., 1997. Wnt signaling and an APC-related gene specify endoderm in early C. elegans embryos. Cell 90, 707–716.
Rudel, D., Kimble, J., 2001. Conservation of glp-1 regulation and function in nematodes. Genetics 157, 639–654.
Rudel, D., Kimble, J., 2002. Evolution of discrete Notch-like receptors from a distant gene duplication in *Caenorhabditis*. Evol. Dev. 4, 319–333.
Salser, S.J., Kenyon, C., 1992. Activation of a C. elegans Antennapedia homologue in migrating cells controls their direction of migration. Nature 355, 255–258.
Salser, S.J., Loer, C.M., Kenyon, C., 1993. Multiple HOM-C gene interactions specify cell fates in the nematode central nervous system. Genes Dev. 7, 1714–1724.
Schwarz-Romond, T., Fiedler, M., Shibata, N., Butler, P.J., Kikuchi, A., Higuchi, Y., Bienz, M., 2007. The DIX domain of Dishevelled confers Wnt signaling by dynamic polymerization. Nat. Struct. Mol. Biol. 14, 484–492.
Sharma-Kishore, R., White, J.G., Southgate, E., Podbilewicz, B., 1999. Formation of the vulva in *Caenorhabditis elegans*: a paradigm for organogenesis. Development 126, 691–699.
Shen, K., Fetter, R.D., Bargmann, C.I., 2004. Synaptic specificity is generated by the synaptic guidepost protein SYG-2 and its receptor, SYG-1. Cell 116, 869–881.
Siegfried, K.R., Kimble, J., 2002. POP-1 controls axis formation during early gonadogenesis in C. elegans. Development 129, 443–453.
Sommer, R. J., 2005. Evolution of development in nematodes related to *C. elegans*. WormBook. ed. The *C. elegans* Research Community, WormBook. doi:10.1895/wormbook.1.46.1, http://www.wormbook.org.
Sommer, R.J., Sternberg, P.W., 1996. Apoptosis and change of competence limit the size of the vulva equivalence group in *Pristionchus pacificus*: a genetic analysis. Curr. Biol. 6, 52–59.
Sternberg, P. W., 2005. Vulval development. WormBook. ed. The *C. elegans* Research Community, WormBook. doi:10.1895/wormbook.1.6.1, http://www.wormbook.org.
Sternberg, P.W., Horvitz, H.R., 1988. lin-17 mutations of Caenorhabditis elegans disrupt certain asymmetric cell divisions. Dev. Biol. 130, 67–73.
Sundaram, M.V., 2005. The love-hate relationship between Ras and Notch. Genes Dev. 19, 1825–1839.
Thorpe, C.J., Schlesinger, A., Carter, J.C., Bowerman, B., 1997. Wnt signaling polarizes an early C. elegans blastomere to distinguish endoderm from mesoderm. Cell 90, 695–705.
Tian, H., Schlager, B., Xiao, H., Sommer, R.J., 2008. Wnt signaling induces vulva development in the nematode *Pristionchus pacificus*. Curr. Biol. 18, 142–146.
Whangbo, J., Kenyon, C., 1999. A Wnt signaling system that specifies two patterns of cell migration in *C. elegans*. Mol. Cell 4, 851–858.
Widelitz, R., 2005. Wnt signaling through canonical and non-canonical pathways: recent progress. Growth Factors 23, 111–116.
Winston, W.M., Sutherlin, M., Wright, A.J., Feinberg, E.H., Hunter, C.P., 2007. *Caenorhabditis elegans* SID-2 is required for environmental RNA interference. Proc. Natl Acad. Sci. USA 104, 10565–10570.
Wood, W.B. (Ed.), 1988. The Nematode *Caenorhabditis elegans*. Cold Spring Harbor Laboratory Press, Cold Spring Harbor New York.
Yu, H., Seah, A., Herman, M.A., Ferguson, E.L., Horvitz, H.R., Sternberg, P.W., 2009. Wnt and EGF pathways act together to induce C. elegans male hook development. Dev. Biol. 327, 419–432.
Zheng, M., Messerschmidt, D., Jungblut, B., Sommer, R.J., 2005. Conservation and diversification of Wnt signaling function during the evolution of nematode vulva development. Nat. Genet. 37, 300–304.